



# OPEN Menin inhibitor MI-503 exhibits potent anti-cancer activity in osteosarcoma

Shen Tian<sup>1,5</sup>, Zhuang-Yu Hao<sup>1,5</sup>, Deng-Hui Xu<sup>2,5</sup>, Xuan-Zong Wang<sup>1</sup>, Cheng-Cheng Shi<sup>3</sup>✉ & Yi Zhang<sup>1,4</sup>✉

Small molecule Menin inhibitor recently has emerged as a new therapeutic by targeting the interaction of histone methyltransferase MLL1 (KMT2A) with Menin. MLL1 is associated with aggressive osteosarcoma (OS) in young adults. The purpose of the study is to explore whether Menin inhibitors have therapeutic effects in OS. To investigate the anti-OS activity of the Menin inhibitor MI-503 in vitro, we performed CCK-8 cell growth and colony formation assay. Cellular thermal shift assay was used to test whether MI-503 binds to Menin in osteosarcoma cells. The expression of oncogenes in MI-503 treated cells were detected by western blotting and Quantitative reverse transcription polymerase chain reaction (RT-qPCR) assay. Finally, we established the OS subcutaneous xenograft mice model to study the anti-OS effect of MI-503 in vivo. The results showed that MI-503 dose-dependently suppressed cell proliferation in 6 OS cell lines, including 143B, HOS, Saos-2, SKES1, MG-63, and U2OS. 143B is the most sensitive cell line with EC50 value 0.13  $\mu$ M. Cellular thermal shift assay showed that MI-503 binds cellular Menin. RT-qPCR assay showed that MI-503 suppressed the expression of Mcl-1 and c-Myc in 143B cells. Western blotting result showed that MI-503 markedly suppressed the H3K4 methylation, significantly suppressed the expression of Mcl-1 and c-Myc, and increased the expression of p27 and cl-PARP in 143B and Saos-2 cells. In a study with 143B cell-derived xenograft model, we found that MI-503 profoundly inhibited OS tumor growth in mice. Immunohistochemistry (IHC) study showed that MI-503 suppressed the H3K4 methylation and inhibited the expression of the cell proliferation biomarker Ki67 in 143B OS xenograft tissue. Overall, our findings demonstrated the potent anti-OS activity of MI-503 in both in vitro and in vivo models, which also indicated that Menin inhibitor may be a prospective therapeutic strategy for human OS.

**Keywords** Histone methylation, Menin, MI-503, Osteosarcoma, Small molecule

Osteosarcoma (OS) is the most common type of bone cancer, with a high morbidity rate in young adults and adolescents, accounting for approximately 19% of all malignant bone tumors and about 5% of all childhood tumors<sup>1–3</sup>. Despite advances in therapeutic strategies that combine chemotherapy, surgery, and sometimes radiotherapy, the prognosis for patients with recurrent or metastatic osteosarcomas remains poor<sup>4</sup>. Chemotherapy, often including drugs such as high-dose methotrexate, doxorubicin, cisplatin, and ifosfamide, is used as neoadjuvant treatment to reduce tumor size before surgery and as adjuvant treatment to mitigate the risk of recurrence. However, its effectiveness in advanced or metastatic OS is limited, with many patients developing resistance to chemotherapy over time<sup>4</sup>. Surgical intervention, which may involve limb salvage or amputation, remains the primary treatment for localized OS. Yet, surgery is not always feasible, especially when tumors are located in functionally critical or surgically inaccessible areas<sup>5</sup>. Furthermore, even with complete surgical resection, the risk of local recurrence and distant metastasis remains high, underscoring the need for more effective treatment strategies<sup>6</sup>. Targeted therapies and immunotherapies are emerging as promising approaches for OS, particularly in the context of advanced or metastatic disease<sup>7</sup>. However, the heterogeneity of OS and the complexity of its underlying molecular mechanisms present challenges in identifying effective targets and predicting treatment response<sup>8</sup>. Heretofore, patients with relapse or metastasized lesions still lack effective

<sup>1</sup>Department of Orthopedics, The First Affiliated Hospital of Zhengzhou University, Zhengzhou, Henan, China.

<sup>2</sup>Department of Emergency, The First Affiliated Hospital of Zhengzhou University, Zhengzhou, Henan, China.

<sup>3</sup>Department of Pharmacy, The First Affiliated Hospital of Zhengzhou University, No.1, East Jian She Road, Zhengzhou 450052, Henan, China. <sup>4</sup>Translational Medicine Center, The First Affiliated Hospital of Zhengzhou University, Zhengzhou, Henan, China. <sup>5</sup>Shen Tian, Zhuang-Yu Hao and Deng-Hui Xu should be considered joint first author. ✉email: fccshicc@zzu.edu.cn; zhangyi@zzu.edu.cn

treatment. These highlight the urgency of exploring novel therapeutic approaches for this lethal disease<sup>9</sup>. Targeting epigenetic dysregulation has drawn increasing attention in cancer treatment and research in the last couple of decades<sup>10–13</sup>.

Histone 3 lysine 4 (H3K4) methylation is a critical epigenetic modification that plays a significant role in the regulation of gene transcription<sup>14</sup>. This modification is dynamically modulated by histone methyltransferases (HMTs) and demethylases, and any imbalance in their activities can lead to the misregulation of H3K4 methylation, which has been implicated in various human cancers<sup>15</sup>. H3K4 methylation has been shown to influence the expression of genes involved in cellular proliferation, differentiation, and apoptosis<sup>16</sup>. Aberrant H3K4 methylation, often resulting from mutations or overexpression of H3K4 methyltransferases such as MLL1, NSD2, and NSD3, can drive oncogenic pathways and contribute to uncontrolled cell proliferation. Therefore, understanding the role of H3K4 methylation in OS is crucial for developing targeted therapies that aim to restore the normal epigenetic balance and inhibit tumor growth. MLL1 (KMT2A) is an epigenetic oncogene. Through interaction with Menin, MLL1 participates in the methylation of histone H3 lysine 4 (H3K4), and leading to transcription of oncogenes<sup>17</sup>. Targeting the interaction by small molecule inhibitors (Menin inhibitors) could overturn the methyltransferase activity of MLL1, thus eliciting anticancer activity in leukemia, breast, prostate, colorectal cancer, and several other types of cancer<sup>18–20</sup>. MLL1 (KMT2A) was reported to have an oncogenic role in OS, however, whether Menin inhibitors have therapeutic effect remains to be studied<sup>21–23</sup>. In this study, we assessed the anti-OS potential of Menin inhibitor MI-503 and investigated the possible underlying mechanisms through both in vitro and in vivo models.

## Materials and methods

### Agents and cell lines

We obtained 6 human OS cell lines from the China Center for Type Culture Collection (Wuhan, China), including 143B, HOS, Saos-2, SKES1, MG-63, and U2OS. These OS cell lines were preserved in PRMI640 or DMEM medium (Thermo Fisher Scientific, Beijing, China)<sup>24</sup>. All of these cell lines were authenticated and cytogenetically tested before being frozen. After thawing from the frozen state, each cell line should be cultured in medium for no more than 8 weeks.

MI-503 was purchased from Selleck Chemicals Shanghai (Shanghai, China). To obtain MI-503 at a concentration of 20 mg/ml, we dissolved it in a suitable volume of dimethyl sulfoxide (DMSO) (Biosharp, China) and then stored it at -80 °C.

### CCK-8 cell growth assay

The Cell Counting Kit-8 was purchased from Sigma-Aldrich (cat# 96992; Shanghai, China), which was used to measure cell growth by obtaining optical density (OD) values as previously described<sup>24,25</sup>. OS cells were suspended in a suitable volume of culture medium, and then 200 µl of cell suspension was added to 96-well plates containing 1000–2000 osteosarcoma cells per well. After cell adhesion, the medium was changed and the OS cells were treated with 0.01, 0.03, 0.1, 0.3, 1, 3, or 10 µM MI-503 for 7 days. Three replicate experiments were performed for all experimental concentrations (n = 3). Then, we incubated each well with 20 µl CCK-8 reagent for 2 h and recorded the absorbance using a microplate reader at 450 nm wavelength.

### Colony formation assay

We performed colony formation assay as described previously<sup>25</sup>. OS 143B and Saos-2 cells were suspended in culture medium and plated in 6-well plates (1000 cells/well), grown overnight, then treated with MI-503 at 0.1, 0.3, and 1 µM for 14 days. DMSO was used as a treatment control. The plates were fixed and dyed with paraformaldehyde and crystal violet successively, then pictures of the plates were taken with a camera. Colonies consisting of more than 50 cells were manually counted. The assays were performed for three times (n = 3). The colony numbers were plotted in the right two panels with GraphPad Prism 9 software.

### Western blotting

We carried out western blotting according to previous method<sup>24</sup>. Treated cells were lysed in Radio Immunoprecipitation Assay (RIPA) lysis buffer (PBS containing 0.5% Na-deoxycholate, 1% NP40, and 0.1% SDS) containing 1 protease inhibitor cocktail tablet and 1 µM phenylmethylsulfonyl fluoride per 10 ml. All operations need to be carried out on ice. The protein concentration of the lysate was determined by the Bio-Rad protein assay kit (cat# 5000001, Shanghai, China)<sup>26</sup>. Different proteins were separated using 8–15% SDS-PAGE gels. We then transferred them onto polyvinylidene difluoride (PVDF) membranes. After blocking them in 5% skim milk for 1 h, the PVDF membranes were exposed to specific primary antibodies, rinsed, and soaked in horseradish peroxidase-conjugated secondary antibody diluent (GE Healthcare, Beijing, China)<sup>27</sup>. The treated PVDF membranes were then visualized using chemiluminescent horseradish peroxidase antibody (n = 3) (Denville Scientific, Guangzhou, China).

We purchased the Menin (#6891), PARP (#9532), Histone 3 (#4499), H3K4me1 (#5326), H3K4me2 (#9725), H3K4me3 (#9751) antibodies from Cell Signaling Technology; c-Myc (9E10)(sc-40), Mcl-1 (S-19) (sc-819), and Tubulin (sc-5274) antibodies were obtained from Santa Cruz Biotechnology (Shanghai, China).

### Cellular thermal shift assay (CETSA)

Briefly,  $2 \times 10^6$  143B cells in DMEM containing 10% fetal bovine serum were seeded in 60 mm dishes in a suitable volume and cultured overnight (5% CO<sub>2</sub>, 37 °C). After attachment, cells were treated with 0.1, 0.3, or 1 µM MI-503 for 1 h at 5% CO<sub>2</sub>, 37 °C (n = 3). Then the cells were collected and rinsed with PBS<sup>24</sup>. Next, cells were resuspended in PBS into 200 µl tubes and then were heated at 45° for 3 min. Cooling these tubes at normal temperature for 3 min and cells were lysed by addition of PBS (50 µl) using liquid nitrogen through 3 cycles of

freeze-thawing. After centrifuging the lysates at 4 °C for 20 min at 20,000 g, the supernatant liquid was moved to new tubes and the result was analyzed by western blotting<sup>28,29</sup>.

### H3K4 methylation assay

Histone was extracted from treated cells with Histone Extraction Kit (cat# ab113476, Abcam, Shanghai, China). Western blotting and specific antibodies were used to examine the expression of H3K4me1, H3K4me2, and H3K4me3. We used Histone 3 as a loading control (n = 3).

### Quantitative reverse transcription polymerase chain reaction (RT-qPCR)

OS 143B cell line was incubated with 1 μM of MI-503 for 24, 48, or 72 h (n = 3). Collecting cells and Trizol was used to extract total RNA from the treated cells and reverse transcribed into cDNA using the HiScript II Q RT SuperMix (cat# R223-01; Vazyme Biotech, Nanjing, China). Following the instructions, qPCR assay was carried out using the ChamQ Universal SYBR qPCR Master Mix (cat# Q711-02; Vazyme Biotech, Nanjing, China)<sup>30</sup>. The reaction conditions were 95 °C for 30 s, 95 °C for 10 s, and 60 °C for 30 s (40 cycles). Tubulin was used to normalize the expression of mRNA. The expression of target gene was quantified by the  $2^{-\Delta\Delta CT}$  approach. The primers used for qPCR were as follows: c-Myc-F: 5'-GTCAAGAGGCGAACACACAAC-3'; c-Myc-R: 5'-TTGGACGGACAGGATGTATGC-3'; Mcl-1-F: 5'-TTCGAAACTGGACATCAAA-3'; Mcl-1-R: 5'-CCACAAAGGCA CCAA AAGA-3'; Tubulin-F: 5'-ACACGGATGAGACCTACT-3'; Tubulin-R: 5'-TGTTCTTGCTCTGGATGG -3'.

### Immunohistochemistry (IHC)

We obtained tumor tissues from tumor-bearing mice treated with MI-503 for 13 days (n = 3). The antibodies H3k4me3 (#9751) and Ki67 (#9449) used for IHC were purchased from Cell Signaling Technology. The experiment was performed according previously described. We first dewaxed these slices with xylene and then rehydrated them in graded concentrations of ethano<sup>31</sup>. These slices have also been boiled in antigen retrieval buffer (Abcam, Shanghai, China) for 5 min in the microwave oven<sup>24</sup>. Next, we soaked the slices into the specific primary antibody diluent for 2 h at room temperature, rinsed them three times with PBS, then soaked them into a horseradish peroxidase-conjugated secondary antibody diluent for 30 min at normal temperature. Slices were subsequently incubated with avidin-biotin complex (Vectorlabs, Shanghai, China) for 30 min and visualized by 3,3'-diaminobenzidine tetrahydrochloride (DAB) reagent (Dako Diagnostics, Shanghai, China). Then the slices were stained with hematoxylin and dehydrated through a series of graded alcohol to xylene<sup>24</sup>. The pictures of the stained slices were then captured by a light microscope (Supplementary Fig. 1).

### Animal studies

6-week-old female BALB/c mice were obtained from Charles River (Beijing, China). Mice were cared for according to NIH guidelines for laboratory animals. The study was carried out in compliance with the ARRIVE guidelines. Animal experiments were approved by the Clinical Trials and Research Ethics Committee of the First Affiliated Hospital of Zhengzhou University (2023-KY-0577). We prepared 143B cells and suspended them in Matrigel (50 million cells/ml). Then the Matrigel (0.1 ml/tumor) was injected subcutaneously into the flank of 6-week-old female BALB/c mice (Charles River, Beijing, China)<sup>25</sup>. To study the in vivo efficacy of MI-503, mice were randomly divided into control or treatment groups (n = 5) when tumors reached about 100 mm<sup>3</sup>. MI-503 (dissolved in vehicle) or vehicle control (25%DMSO, 25%PEG400, 50%PBS) was administrated intraperitoneal injection (10 mg/kg MI-503 or the same volume of vehicle) every 2 days for 13 days. Animal tumor volume and weight were measured every 2 days. To calculate the tumor volume, we used Tumor volume (mm<sup>3</sup>) = (length × width<sup>2</sup>)/2.  $TGI = (V_c - V_t)/(V_c - V_o) \times 100$  was used to calculate tumor growth inhibition.  $V_c$  is the median of the control group and  $V_t$  is the median of the treated group at the end of the study,  $V_o$  is the median at the start of the study<sup>24</sup>. After 13 days of treatment, all mice were euthanized by intravenous injection of pentobarbital sodium at a dose of 200 mg/kg and tumor tissues were collected<sup>25</sup>. The expression of H3K4m3 and Ki67 in tumor tissues were analyzed through IHC.

### Statistical analysis

We repeated each experiment three times independently. The results were shown as the mean ± SE<sup>24</sup>. Unpaired t-test and ANOVA test were used for statistical analysis. The results with  $p < 0.05$  were considered significant, which are specified in the text or figure legends.

### Agents and cell lines

All cell lines were authenticated and tested for mycoplasma contamination before being used in the experiments. Mycoplasma testing was performed using the MycoAlert Mycoplasma Detection Kit (Vazyme, China) following the manufacturer's instructions, and all cell lines were confirmed to be mycoplasma-free.

## Results

### MI-503 potently suppresses OS cell proliferation

We first assessed the antiproliferative effect of MI-503 through CCK-8 assay in 6 OS cell lines, including 143B, HOS, Saos-2, SKES1, MG-63, and U2OS. The results revealed that after treated for 7 days, MI-503 potently and dose-dependently inhibited cell proliferation in all 6 OS cell lines with low micromolar EC50 values (Fig. 1A). OS cell lines with mutated p53, such as 143B, HOS, and Saos-2 are extraordinarily sensitive to MI-503 with EC50 values of 0.13, 0.16, and 0.29 μM, respectively<sup>24,32</sup>. In contrast, OS cell lines with wild-type p53, including SKES1, MG-63, and U2OS show relative weaker sensitive to MI-503, with EC50 values 0.89, 2.1, and 1.2 μM, respectively (Fig. 1A).

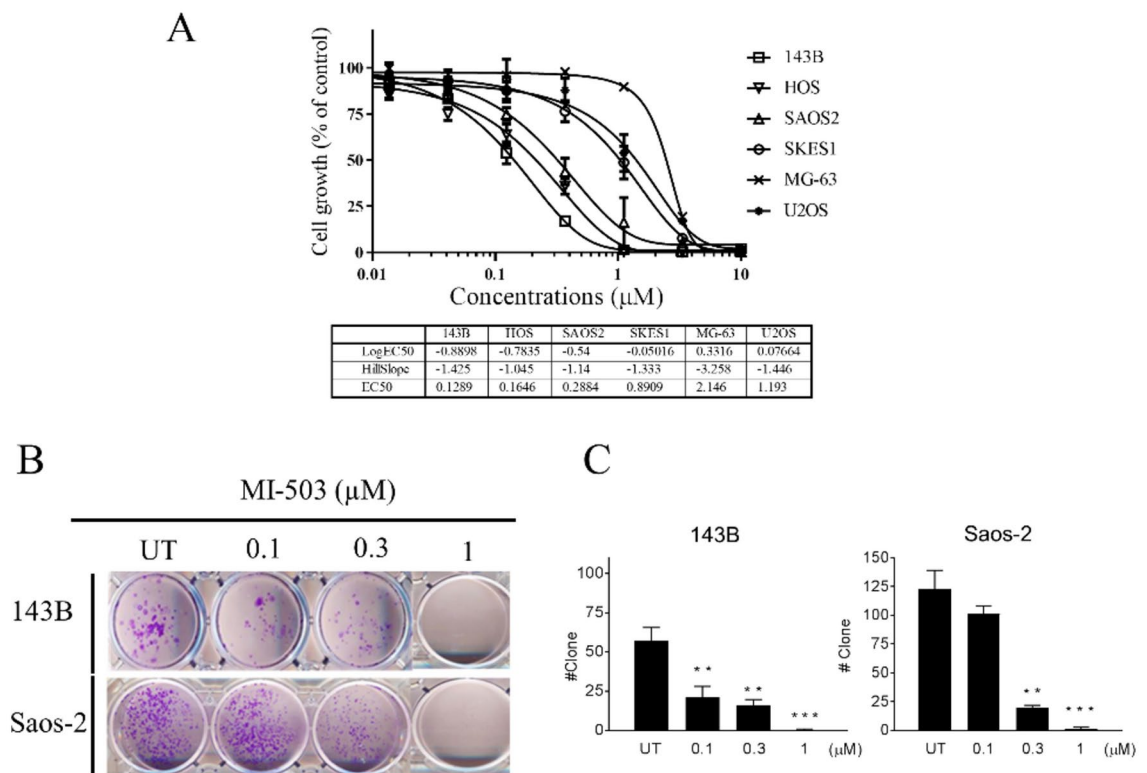


**Fig. 1.** MI-503 suppresses the proliferation of OS cells in vitro. **(A)** Dose-dependent inhibition of cell growth in OS cell lines treated with MI-503 for 7 days, as measured by CCK-8 assay **(B)** The clone formation experiment showed that MI503 inhibited the growth of 143B and Saos-2 cells **(C)** Colonies consisting of more than 50 cells were counted. \*\* $p < 0.001$ , \*\*\* $p < 0.0001$ .

For testing a longer-term antiproliferative activity, we carried out clonogenic formation assay in 143B and Saos-2, two sensitive OS cell lines. The results showed that treatment with MI-503 at 0.1, 0.3, and 1 μM for 14 days markedly and dose-dependently attenuated the ability to form clones in both cell lines ( $p < 0.05$  for all comparisons). Noticeably, in both cell lines, MI-503 at 1 μM completely blocked the cells to form clones (Fig. 1B,C).

These results demonstrated that MI-503 has a potent ability to inhibit OS cell proliferation in vitro.

### MI-503 binds Menin protein and suppresses H3K4 methylation in OS cells

Cellular thermal shift assay (CETSA) is a new research skill used to detect target engagement by a ligand<sup>28,29,33</sup>. A recent study showed that MI-503 is able to protect Menin from 45 °C heating-induced protein melting<sup>28,29</sup>. To examine whether the antiproliferative activity in OS cells is associated with Menin targeted by MI-503, we treated 143B cells with MI-503 at 0.1, 0.3, and 1 μM for 1 h, then examined the cellular thermal sensitive of Menin protein in treated cells to 45 °C heating. We observed that compared to DMSO treatment, MI-503 protected Menin from heating in a dose-dependent approach ( $p < 0.01$  for 0.1 μM,  $p < 0.001$  for 0.3 μM and 1 μM). The results indicated that MI-503 binds to Menin in OS cells. (Fig. 2A)<sup>34</sup>.

The inhibition of MLL1-Menin interaction by MI-503 is designed to repress the methyltransferase activity of MLL1 on H3K4<sup>34</sup>. We next researched the effect of MI-503 on the methylation of H3K4. The results showed that treatment with MI-503 at 0.1, 0.3, and 1 μM for 48 h distinctly inhibited tri-methylation of H3K4 in a dose-dependent manner. The same treatments also markedly inhibited the mono- and di-methylation of H3K4 (Fig. 2B). ( $p < 0.05$  for mono- and di-methylation,  $p < 0.001$  for tri-methylation).

### Inhibition of Menin by MI-503 suppresses the expression of oncogene in OS cells

We next investigated the inhibition of H3K4 methylation could lead to repression of the expression of c-Myc and Mcl-1, two genes which have been reported sustained by MLL1-Menin interaction<sup>32,35–37</sup>. Our results of RT-qPCR study showed that MI-503 treatment significantly suppressed the expression of c-Myc and Mcl-1 mRNA in 143B cells (Fig. 2C,D)<sup>37,38</sup>. Western blotting assay indicated that the transcription inhibition of these two oncogenes transfer to the decrease of protein level, and also decreased the level of p27 in the OS cells ( $p < 0.05$  for all comparisons) (Fig. 3)<sup>39,40</sup>. The results of western blotting also indicated that the expression of cleaved PARP (cl-PARP) was significantly increased after the MI503 treatment, especially at a concentration of 1 μM, which has been reported to be closely associated with DNA damage repair and apoptosis<sup>41</sup>. These results collectively demonstrated that targeting MLL1-Menin interaction by MI-503 profoundly inhibited H3K4 methylation and finally led to the suppression of oncogenes.

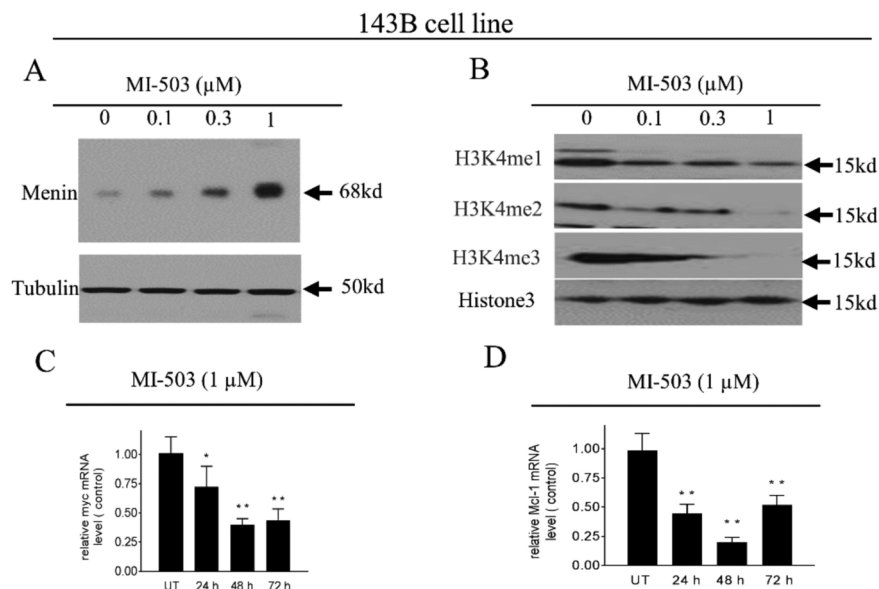


**Fig. 2.** MI-503 binds Menin protein, reduces H3K4 methylation and induces transcriptional repression in OS cells. **(A)** Results from the CETSA performed in 143B cells. Compared to DMSO treatment, MI-503 protected Menin from heating in a dose-dependent approach **(B)** Treatment with MI-503 at 0.1, 0.3, and 1 μM for 48 h distinctly inhibited tri-methylation of H3K4 in a dose-dependent manner. The same treatments also markedly inhibited the mono- and di-methylation of H3K4 **(C,D)** 143B cells line was treated with MI-503 at 1 μM as indicated for 24, 48, and 72 h. MI-503 treatment significantly suppressed the expression of c-Myc and Mcl-1 mRNA in 143B cells \* $p < 0.01$ , \*\* $p < 0.001$ .

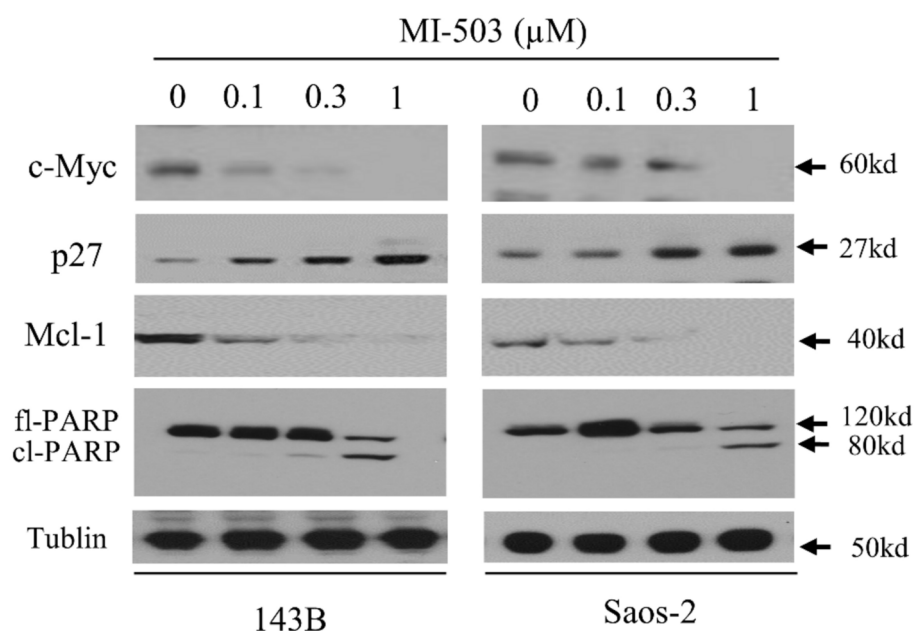


**Fig. 3.** Inhibition of Menin by MI-503 suppresses the expression of oncogenic proteins in OS cells. **(A)** The transcription inhibition of c-Myc and Mcl-1 transfer to the decrease of protein level, and also decreased the level of p27 in the OS cells ( $p < 0.05$  for all comparisons). The expression of cleaved PARP (cl-PARP) was significantly increased after the MI503 treatment. These results collectively demonstrated that targeting MLL1-Menin interaction by MI-503 profoundly inhibited H3K4 methylation and finally led to the suppression of oncogenes.



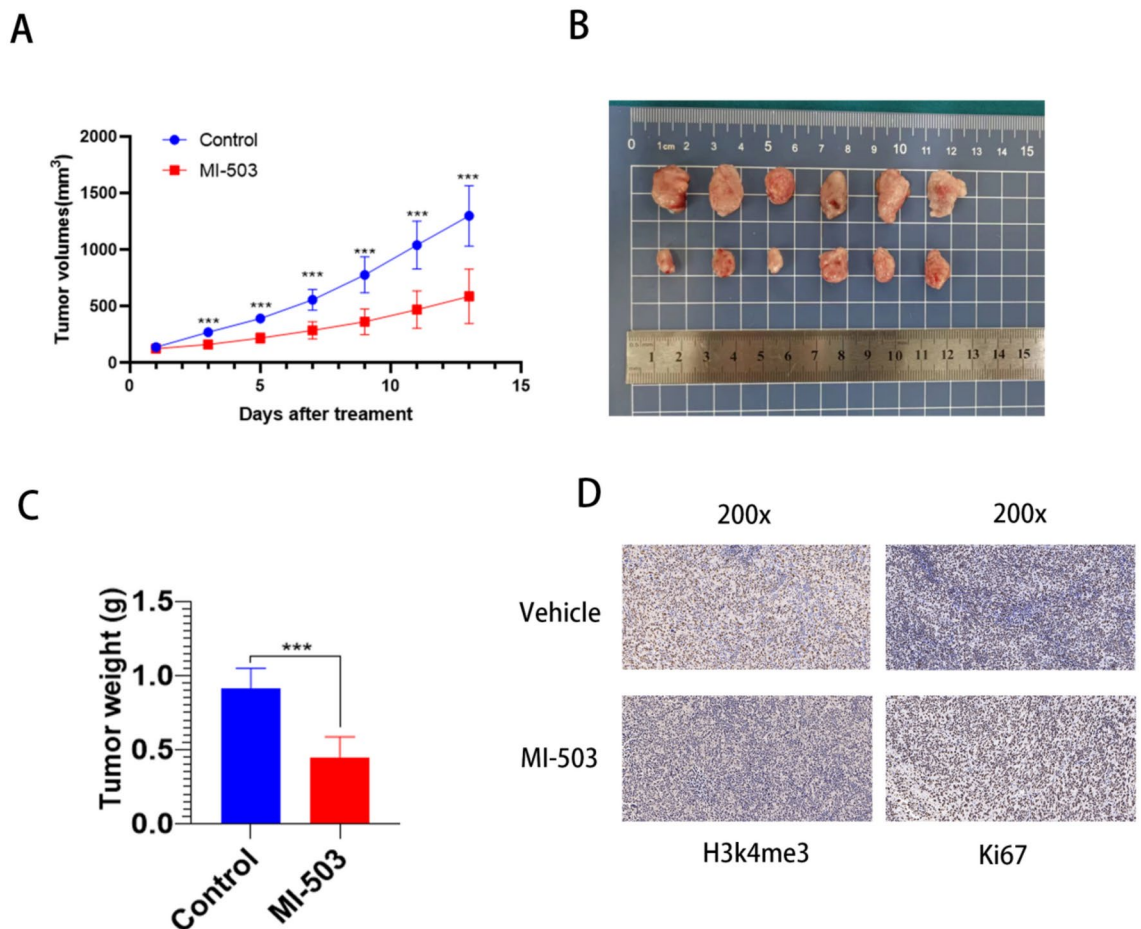


**Fig. 4.** Menin inhibitor MI-503 significantly inhibits tumor growth of OS 143B xenografts in mice. **(A)** The overall tumor volume of the MI-503 group is smaller than that of the vehicle group **(B)** Mice bearing 143B xenograft tumor were euthanized at 13 days. **(C)** Tumor values were compared with *t*-test between the two groups. The tumor weight in the MI-503 group is lighter than that in the vehicle group **(D)** The expression of H3K4me3 and Ki67 were examined by IHC with specific antibodies. \*\*\**p* < 0.001.

#### MI-503 inhibits tumor growth in 143B OS xenografts in mice and suppresses tri-methylation of H3K4 and Ki67 in xenograft tissue

We finally researched the anti-tumor efficacy of MI-503 in a subcutaneous OS xenograft mouse model with 143B, the most sensitive cell line<sup>24</sup>. Intraperitoneal injection of MI-503 at 10 mg/kg for 13 days led to significant inhibition of tumor growth (Fig. 4A–C). Notably, after 2 doses, tumors in MI-503 treated group are significantly smaller than those treated by vehicle ( $162.28 \pm 29.48 \text{ mm}^3$  vs  $270.79 \pm 31.43 \text{ mm}^3$ ,  $p < 0.0001$ ). As the treatment continuing, the difference of tumor volume between the two groups gradually enlarges. On day 13, the average tumor volume reached  $1298.59 \pm 267.42 \text{ mm}^3$  in vehicle group. In contrast, the average tumor volume in MI-503 group was only  $587.19 \pm 240.69 \text{ mm}^3$ , highly significant smaller than that in vehicle group ( $p < 0.0001$ ) (Fig. 4A). This demonstrated that MI-503 therapy shows strong efficacy in OS xenograft tumor.

IHC staining assay demonstrated that after dosing MI-503 for 13 days, H3K4 tri-methylation was markedly suppressed in 143B OS xenograft tissue (Fig. 4D). Moreover, we further employed IHC to analyze the expression of Ki67 in the tumor tissue<sup>42</sup>. The results showed that MI-503 treatment distinctly decreased the percentage of cells positively stained by Ki67 ( $p < 0.01$ ) (Fig. 4D). These results suggested that the strong efficacy of MI-503 in OS tumor may be attributed to the anti-proliferative activity in tumor tissue.

#### Discussion

MLL1 is a newly identified epigenetic protein with oncogenic function. Through catalyzing the H3K4 methylation, MLL1 plays a role in sustaining the expression of a series of oncogene through transcription<sup>17,34,43</sup>. Three decades ago, it was found that chromosomal rearrangements in the MLL locus appeared in certain subtypes of acute lymphoblastic leukemia (ALL) and acute myeloid leukemia (AML). MLL rearrangements leads to MLL gene fusion, which in turn leads to pathogenesis and more aggressive phenotypes in these two diseases<sup>18,44,45</sup>. Of note, the oncogenic function of MLL1 in lysine methyltransferases relies on the interaction of MLL1 with Menin protein. Accordingly, inhibition of the MLL1-Menin protein–protein interaction by small molecules has been persuaded as a novel therapeutic strategy for these leukemia. Heretofore, preclinical studies demonstrated that

several series of Menin inhibitors, including MI-503, have strong anti-cancer activity in AML and ALL<sup>18,43,44</sup>. Interestingly, recent studies revealed that besides these two types of leukemia, breast, ovarian, lung, prostate, and many other types of cancer are also sensitive to Menin inhibitors<sup>28,29,46</sup>. Importantly, several Menin inhibitors have been under clinical trials and show promising efficacy in acute leukemia.

In this study, in order to explore a novel therapy for patients with advanced OS, the most common type of bone cancer, we expanded the anticancer study of this new drug in OS cells. Through in vitro cell proliferation, clonogenic analysis, and also in vivo study, our data strongly suggested that the Menin inhibitors may also have potent anticancer activity in OS. In comparison to current OS treatments, such as chemotherapy and surgery, MI-503 offers several potential advantages. Firstly, MI-503 has demonstrated high oral bioavailability (75%) and achieves high levels in peripheral blood following a single intravenous or oral dose<sup>47</sup>. Secondly, MI-503 has shown strong inhibition of tumor growth with once-daily intraperitoneal administration, leading to an over 80% reduction in tumor volume and complete tumor regression in some cases<sup>18</sup>. Lastly, MI-503 treatment has resulted in markedly reduced expression of Hoxa9 and Meis1, downstream targets of MLL fusion proteins that are substantially upregulated in MLL leukemias<sup>18</sup>. These advantages suggest that MI-503 may provide a more targeted and effective treatment option for OS, particularly in cases where traditional therapies have failed or are not suitable. Our these findings, together with the information of previous investigations, indicated that Menin inhibitors may be a novel drug in broad types of cancer in the near future.

Mechanistically, our study revealed that OS cell lines with mutated p53 are more sensitive to the Menin inhibitor than cell lines with wild-type p53. The p53 status, whether wild-type or mutant, significantly influences treatment outcomes in OS. Wild-type p53 expressing tumors are generally more sensitive to DNA-damaging agents, as p53 can induce cell cycle arrest, apoptosis, and senescence, which are crucial for the effectiveness of chemotherapy and radiation therapy<sup>48,49</sup>. In contrast, tumors with mutant p53 often exhibit resistance to these treatments, as the loss of p53 function can lead to uncontrolled cell proliferation and evasion of apoptosis<sup>50</sup>. Moreover, the anti-OS activity of the Menin inhibitor is associated with cellular Menin targeting, thereof the inhibition of H3K4 methylation, the suppression of oncogenes c-Myc, Mcl-1 and p27, and increased the expression of cl-PARP. These findings substantiated the findings by Shin et al. that OS cells with defective p53 function rely on RUNX2-Menin/MLL1-Histone3K4 methylation-Myc axis for survival than the p53 wild-type cells<sup>52</sup>. Inhibition of histone3K4 methylation by a Menin inhibitor disturbs this survival axis. Nevertheless, whether and how the RUNX2-Menin/MLL1-Histone3K4 methylation-Myc axis also controls the expression of Mcl-1, p27 and other oncogenes remains to be further investigated.

In this study, we utilized in vitro and xenograft models to evaluate the efficacy of MI-503 in osteosarcoma (OS). While these models have been instrumental in identifying potential therapeutic agents and understanding tumor biology, they are not without limitations. Cell lines provide a controlled environment for studying drug effects and toxicities. However, they may not fully represent the heterogeneity and complexity of tumors found in patients. Xenograft models do not provide information about the initiation and etiology of OS, as they utilize fully immortalized OS cells<sup>51</sup>. Furthermore, the ectopic inoculation of cells under the skin may not accurately reflect the tumor's behavior in its natural bone environment. Orthotopic OS models, which involve the implantation of cells directly into bone, may offer more relevant preclinical data, as they better simulate the natural progression and metastatic potential of OS<sup>52</sup>. Moreover, patient-derived xenograft (PDX) models, which involve the transplantation of patient tumor tissue into immunodeficient mice, have been shown to closely mimic the genetic and histologic characteristics of the original tumors. In conclusion, while our in vitro and xenograft models suggest the potential efficacy of MI-503 in OS, these findings should be interpreted with caution due to the inherent limitations of these models<sup>18</sup>. Future studies utilizing orthotopic and PDX models will be essential to further validate the clinical relevance of our results.

In summary, our study demonstrated Menin inhibitors are able to inhibit H3K4 methylation by targeting cellular Menin protein in OS cells in culture and in tumor tissue. This led to the suppression of a few oncogenes, and thus finally resulting in potent anti-OS activity. Overall, our study facilitated the exploration of novel therapy for OS.

## Data availability

All results of this study have been shown in the article. If you want more information, please contact the corresponding author. This article doesn't use the database.

Received: 28 May 2024; Accepted: 19 February 2025

Published online: 27 February 2025

## References

1. Beird, H. et al. Osteosarcoma. *Nat. Rev. Dis. Primers* **8**(1), 77 (2022).
2. Gill, J. & Gorlick, R. Advancing therapy for osteosarcoma. *Nat. Rev. Clin. Oncol.* **18**(10), 609–624 (2021).
3. Ottaviani, G. & Jaffe, N. The epidemiology of osteosarcoma. *Cancer Treat. Res.* **152**, 3–13 (2009).
4. Goorin, A. M. et al. Presurgical chemotherapy compared with immediate surgery and adjuvant chemotherapy for nonmetastatic osteosarcoma: Pediatric Oncology Group Study POG-8651. *J. Clin. Oncol.* **21**(8), 1574–1580 (2003).
5. Winkler, K. et al. Neoadjuvant chemotherapy of osteosarcoma: results of a randomized cooperative trial (COSS-82) with salvage chemotherapy based on histological tumor response. *J. Clin. Oncol.* **6**(2), 329–337 (1988).
6. Meyers, P. A. et al. Chemotherapy for nonmetastatic osteogenic sarcoma: the Memorial Sloan-Kettering experience. *J. Clin. Oncol.* **10**(1), 5–15 (1992).
7. Lewis, I. J. et al. Improvement in histologic response but not survival in osteosarcoma patients treated with intensified chemotherapy: a randomized phase III trial of the European Osteosarcoma Intergroup. *J. Natl. Cancer Inst.* **99**(2), 112–128 (2007).
8. Marina, N. et al. International collaboration is feasible in trials for rare conditions: The EURAMOS experience. *Cancer Treat. Res.* **152**, 339–353 (2009).

9. Chen, C. et al. Immunotherapy for osteosarcoma: Fundamental mechanism, rationale, and recent breakthroughs. *Cancer Lett.* **500**, 1–10 (2021).
10. Filippakopoulos, P. et al. Selective inhibition of BET bromodomains. *Nature* **468**(7327), 1067–1073 (2010).
11. Kansara, M. et al. Translational biology of osteosarcoma. *Nat. Rev. Cancer* **14**(11), 722–735 (2014).
12. Lovén, J. et al. Selective inhibition of tumor oncogenes by disruption of super-enhancers. *Cell* **153**(2), 320–334 (2013).
13. Morrow, J. & Khanna, C. Osteosarcoma genetics and epigenetics: Emerging biology and candidate therapies. *Crit. Rev. oncogenes*. **20**, 173–197 (2015).
14. Xiao, C. et al. H3K4 trimethylation regulates cancer immunity: a promising therapeutic target in combination with immunotherapy. *J. Immunother. Cancer* **11**(8), e005693 (2023).
15. Kumar, A. et al. Pathogenic and therapeutic role of H3K4 family of methylases and demethylases in cancers. *Indian J. Clin. Biochem.* **34**(2), 123–132 (2019).
16. Li, Z. F. et al. Hypoxia inducible factor-3 $\alpha$  promotes osteosarcoma progression by activating KDM3A-mediated demethylation of SOX9. *Chem. Biol. Interact* **351**, 109759 (2022).
17. Dreijerink, K., Timmers, H. & Brown, M. Twenty years of menin: emerging opportunities for restoration of transcriptional regulation in MEN1. *Endocrine-Relat. Cancer* **24**(10), T135–T145 (2017).
18. Borkin, D. et al. Pharmacologic inhibition of the Menin-MLL interaction blocks progression of MLL leukemia in vivo. *Cancer Cell* **27**(4), 589–602 (2015).
19. Alexandrova, E. et al. Combinatorial targeting of menin and the histone methyltransferase DOT1L as a novel therapeutic strategy for treatment of chemotherapy-resistant ovarian cancer. *Cancer Cell Int.* **22**(1), 1–13 (2022).
20. Chou, C. W. et al. Menin and menin-associated proteins coregulate cancer energy metabolism. *Cancers* **12**(9), 2715 (2020).
21. Brichard, B. et al. Unusual association of MLL rearrangement and secondary myelomonocytic leukemia in a 15-year-old patient treated for osteosarcoma. *Leukemia Res.* **31**(11), 1597–1599 (2007).
22. Jiang, Y. et al. An evolutionarily conserved mechanism that amplifies the effect of deleterious mutations in osteosarcoma. *Mol. Genet. Genom. MGG* **297**(2), 373–385 (2022).
23. Yoshida, A. et al. KMT2A (MLL) fusions in aggressive sarcomas in young adults. *Histopathology* **75**(4), 508–516 (2019).
24. Shi, C. et al. PROTAC induced-BET protein degradation exhibits potent anti-osteosarcoma activity by triggering apoptosis. *Cell Death Dis.* **10**(11), 815 (2019).
25. Zhang, H. et al. Targeting BET proteins with a PROTAC molecule elicits potent anticancer activity in HCC cells. *Front. Oncol.* **9**, 1471 (2019).
26. Yu, L. & Hales, C. Long-term exposure to hypoxia inhibits tumor progression of lung cancer in rats and mice. *BMC Cancer* **11**, 331 (2011).
27. Zhang, X. et al. Osimertinib (AZD9291), a mutant-selective EGFR inhibitor, reverses ABCB1-mediated drug resistance in cancer cells. *Molecules (Basel, Switzerland)* **21**(9), 1236 (2016).
28. Kempinska, K. et al. Pharmacologic inhibition of the menin-MLL interaction leads to transcriptional repression of PEG10 and blocks hepatocellular carcinoma. *Mol. Cancer Ther.* <https://doi.org/10.1158/1535-7163.MCT-17-0580> (2017).
29. Malik, R. et al. Abstract 3636: Targeting the MLL complex in castration resistant prostate cancer. *Nat. Med.* **21**(4), 3636 (2015).
30. Bai, J. et al. Low level laser therapy promotes bone regeneration by coupling angiogenesis and osteogenesis. *Stem Cell Res. Ther.* **12**(1), 432 (2021).
31. Tan, W. C. C. et al. Overview of multiplex immunohistochemistry/immunofluorescence techniques in the era of cancer immunotherapy. *Cancer Commun.* **40**(4), 135–153 (2020).
32. Shin, M. et al. A RUNX2-mediated epigenetic regulation of the survival of p53 defective cancer cells. *PLoS Genet.* **12**(2), e1005884 (2016).
33. Jafari, R. et al. The cellular thermal shift assay for evaluating drug target interactions in cells. *Nat. Protocols Erecipes Res.* **9**, 2100–2122 (2014).
34. Kempinska, K. et al. PEG10 pharmacologic inhibition of the Menin-MLL interaction leads to transcriptional repression of and blocks hepatocellular carcinoma. *Mol. Cancer Ther.* **17**(1), 26–38 (2018).
35. Zaman, S. et al. FBP1 is an interacting partner of Menin. *Int. J. Endocrinol.* **2014**(30), 535401 (2015).
36. Brès, V. et al. SKIP interacts with c-Myc and Menin to promote HIV-1 Tat transactivation. *Mol. Cell* **36**(1), 75–87 (2009).
37. Zhang, Y. et al. Inhibition of Mcl-1 enhances Pevonedistat-triggered apoptosis in osteosarcoma cells. *Exp. Cell Res.* **358**, 234–241 (2017).
38. Shen, S. et al. CircECE1 activates energy metabolism in osteosarcoma by stabilizing c-Myc. *Mol. Cancer* **19**(1), 151 (2020).
39. Wang, J. et al. The interaction of SKP2 with p27 enhances the progression and stemness of osteosarcoma. *Ann. New York Acad. Sci.* **1490**(1), 90–104 (2021).
40. Li, Y. et al. p27 is a candidate prognostic biomarker and metastatic promoter in osteosarcoma. *Cancer Res.* **76**(13), 4002–4011 (2016).
41. Subramaniam, D. et al. Suppressing STAT5 signaling affects osteosarcoma growth and stemness. *Cell Death Dis.* **11**(2), 149 (2020).
42. Zeng, M. et al. The relationship between the expression of Ki-67 and the prognosis of osteosarcoma. *BMC Cancer* **21**(1), 210 (2021).
43. Bai, H. et al. Menin-MLL protein-protein interaction inhibitors: a patent review (2014–2021). *Expert Opin. Ther. Patents* **32**(5), 507–522 (2022).
44. Krivtsov, A. et al. A Menin-MLL inhibitor induces specific chromatin changes and eradicates disease in models of MLL-rearranged leukemia. *Cancer Cell* **36**(6), 660–673.e11 (2019).
45. Kolomietz, E. et al. Primary chromosomal rearrangements of leukemia are frequently accompanied by extensive submicroscopic deletions and may lead to altered prognosis. *Blood* **97**(11), 3581–3588 (2001).
46. Svoboda, L. et al. Menin regulates the serine biosynthetic pathway in Ewing sarcoma. *J. Pathol.* **245**(3), 324–336 (2018).
47. Lin, T. L. et al. Targeting IGF2BP3 enhances antileukemic effects of menin-MLL inhibition in MLL-AF4 leukemia. *Blood Adv.* **8**(2), 261–275 (2024).
48. Whibley, C., Pharoah, P. D. & Hollstein, M. p53 polymorphisms: cancer implications. *Nat. Rev. Cancer* **9**(2), 95–107 (2009).
49. Marvalim, C., Datta, A. & Lee, S. C. Role of p53 in breast cancer progression: An insight into p53 targeted therapy. *Theranostics* **13**(4), 1421–1442 (2023).
50. Liu, Y. et al. Understanding the complexity of p53 in a new era of tumor suppression. *Cancer Cell* **42**(6), 946–967 (2024).
51. Jin, J. et al. Challenges and prospects of patient-derived xenografts for cancer research. *Cancers (Basel)* **15**(17), 4352 (2023).
52. Tan, L. et al. Advances of osteosarcoma models for drug discovery and precision medicine. *Biomolecules* **13**(9), 1362 (2023).

# Acknowledgements

We thank Henan Key Laboratory of Digestive Organ Transplantation, the First Affiliated Hospital of Zhengzhou University for their help in raising mice. We thank the Translational Medicine Center of the First Affiliated Hospital of Zhengzhou University for providing Experimental conditions.



## Author contributions

Conceptualization, Yi Zhang and Shen Tian; Methodology, Zhuang-Yu Hao and Deng-Hui Xu; Validation, Deng-Hui Xu and Xuan-Zong Wang; Investigation, Cheng-Cheng Shi and Xuan-Zong Wang; Writing—Original Draft, Shen Tian and Zhuang-Yu Hao; Writing—Review & Editing, Yi Zhang and Cheng-Cheng Shi; Visualization, Shen Tian and Zhuang-Yu; Funding Acquisition, Yi Zhang and Cheng-Cheng Shi.

## Funding

This work was supported by Young and Middle-aged Academic Pacemaker of Henan Provincial Health Commission (HNSWJW-2020027), Distinguished Young Scientists Fund of Henan Provincial Health Commission (YXKC2020025), Excellent Young Scientists Fund of Natural Science Foundation of Henan Province (222300420072), National Natural Science Foundation of China (82204521), Excellent Young Scientists Fund of Henan Provincial Health Commission (YXKC2022059).

## Declarations

### Competing interests

The authors declare no competing interests.

### Ethical approval

The research program was approved by the ethics committee: Clinical Trials and Research Ethics Committee of the First Affiliated Hospital of Zhengzhou University (2023-KY-0577). All animals were cared for in a humane manner according to NIH guidelines for laboratory animals. The study was carried out in compliance with the ARRIVE guidelines.

### Consent for publication

All authors agree to be published.

### Additional information

**Supplementary Information** The online version contains supplementary material available at <https://doi.org/10.1038/s41598-025-91351-y>.

**Correspondence** and requests for materials should be addressed to C.-C.S. or Y.Z.

**Reprints and permissions information** is available at [www.nature.com/reprints](http://www.nature.com/reprints).

**Publisher's note** Springer Nature remains neutral with regard to jurisdictional claims in published maps and institutional affiliations.

**Open Access** This article is licensed under a Creative Commons Attribution-NonCommercial-NoDerivatives 4.0 International License, which permits any non-commercial use, sharing, distribution and reproduction in any medium or format, as long as you give appropriate credit to the original author(s) and the source, provide a link to the Creative Commons licence, and indicate if you modified the licensed material. You do not have permission under this licence to share adapted material derived from this article or parts of it. The images or other third party material in this article are included in the article's Creative Commons licence, unless indicated otherwise in a credit line to the material. If material is not included in the article's Creative Commons licence and your intended use is not permitted by statutory regulation or exceeds the permitted use, you will need to obtain permission directly from the copyright holder. To view a copy of this licence, visit <http://creativecommons.org/licenses/by-nc-nd/4.0/>.

© The Author(s) 2025